Biallelic variants in LARS2 and KARS cause deafness and (ovario)leukodystrophy

Marjo S. van Der Knaap, Marianna Bugiani, Marisa Mendes, Lisa Riley, Desiree E.C. Smith, Joëlle Rudinger-Thirion, Magali Frugier, Marjolein Breur, Joanna Crawford, Judith van Gaalen, et al.

Article NEUROLOGY MS ID# NEUROLOGY/2018/926782

Bi-allelic variants in *LARS2* and *KARS* cause deafness and (ovario)leukodystrophy

Marjo S. van der Knaap, MD PhD[1,2]; Marianna Bugiani, MD PhD[3]; Marisa I. Mendes, PhD[4]; Lisa G. Riley, PhD[5]; Desiree E.C. Smith, PhD[4]; Joëlle Rudinger-Thirion, PhD[6]; Magali Frugier, PhD[6]; Marjolein Breur[1,3]; Joanna Crawford, MS[7]; Judith van Gaalen, MD[8]; Meyke Schouten, MD[9]; Marjolaine Willems, MD[10]; Quinten Waisfisz, PhD[11]; Frederic Tran Mau-Them, MD[12]; Richard J. Rodenburg, PhD[13]; Ryan J. Taft, PhD[14]; Boris Keren, MD PhD[15,16]; John Christodoulou, PhD[5,17,18]; Christel Depienne, PhD[16,19]; Cas Simons, PhD[7,17]; Gajja S. Salomons, PhD[4]; Fanny Mochel MD PhD[15,16,20]

[1]Department of Child Neurology, Amsterdam University Medical Centers and Amsterdam Neuroscience, Amsterdam, The Netherlands

[2]Department of Functional Genomics, Center for Neurogenomics and Cognitive Research, VU University, Amsterdam, The Netherlands

[3]Department of Neuropathology, Amsterdam University Medical Centers and Amsterdam Neuroscience, Amsterdam, The Netherlands

[4]Metabolic Unit, Department of Clinical Chemistry, Amsterdam University Medical Centers and Amsterdam Neuroscience, Amsterdam, The Netherlands

[5]Genetic Metabolic Disorders Research Unit, The Children's Hospital at Westmead, and Discipline of Child and Adolescent Health, Sydney Medical School, University of Sydney, Sydney, NSW, Australia

[6]Architecture et Réactivité de l'ARN, UPR 9002, Université de Strasbourg, CNRS, Strasbourg, France

[7]Institute for Molecular Bioscience, University of Queensland, St. Lucia, Queensland, Australia

[8]Department of Neurology, Radboud University Medical Center, Donders Institute for Brain, Cognition and Behaviour, Nijmegen, The Netherlands.

[9]Department of Clinical Genetics, Radboud University Medical Center, Nijmegen, The Netherlands

[10]Departement Génétique Médicale, Maladies Rares et Médecine Personnalisée, Hôpital Arnaud de Villeneuve, CHRU de Montpellier, Montpellier, France

[11]Department of Clinical Genetics, Amsterdam University Medical Centers, Amsterdam, The Netherlands

[12]UF Innovation en Diagnostic Génomique des Maladies Rares, Centre Hospitalier Universitaire de Dijon, Dijon, France

[13] Radboud Center for Mitochondrial Medicine, Translational Metabolic Laboratory, Department of Pediatrics, Radboud University Medical Center, Nijmegen, the Netherlands

[14]Illumina Inc, San Diego, California, USA

[15]AP-HP, La Pitié-Salpêtrière University Hospital, Department of Genetics, Paris, France

[16]INSERM U 1127, CNRS UMR 7225, Sorbonne Universités, UPMC Univ Paris 06 UMR S 1127, Institut du Cerveau et de la Moelle épinière, ICM, Paris, France

[17]Murdoch Children's Research Institute, Parkville, Victoria, Australia.

[18]Department of Paediatrics, University of Melbourne, Melbourne, Australia

[19]Institute of Human Genetics, University Hospital Essen, University Duisburg-Essen, 45147 Essen, Germany

[20] Sorbonne Universités, Neurometabolic Clinical Research Group, Paris, France

Corresponding author: Marjo S. van der Knaap, Department of Child Neurology, VU University Medical Center, De Boelelaan 1117, 1081 HV Amsterdam, The Netherlands. Phone +31-20-4442419, fax +31-20-4440844, email ms.vanderknaap@vumc.nl

Running head: *LARS2, KARS* and mitochondrial leukodystrophy.

Count: Abstract: 250 words; Manuscript: 4495 words; Title: 80 characters; References:50; Tables: 2; Figures: 5.

Search terms: [155] Leukodystrophies; [96] Mitochondrial disorders; [120] MRI.

Study funding: This study was in part financed by the Australian National Health and Medical Research Council (NHMRC 1068278), the Victorian Government's Operational Infrastructure Support Program and the ZonMw grant 40-00812-98-11005. The Genotype-Tissue Expression (GTEx) Project was supported by the Common Fund of the Office of the Director of the National Institutes of Health, and by NCI, NHGRI, NHLBI, NIDA, NIMH, and NINDS.

Authors' Disclosures

Marjo S. van der Knaap reports no disclosure.

Marianna Bugiani reports no disclosure.

Marisa I. Mendes reports no disclosure.

Lisa G. Riley reports no disclosure.

Desiree E.C. Smith reports no disclosure.

Joëlle Rudinger-Thirion reports no disclosure.

Magali Frugier reports no disclosure.

Marjolein Breur reports no disclosure.

Joanna Crawford reports no disclosure.

Judith van Gaalen reports no disclosure.

Meyke Schouten reports no disclosure.

Marjolaine Willems reports no disclosure.

Quinten Waisfisz reports no disclosure.

Frederic Tran Mau-Them reports no disclosure.

Richard J. Rodenburg reports no disclosure.

Ryan J. Taft is an employee of Illumina, Inc.

Boris Keren reports no disclosure.

John Christodoulou reports no disclosure.

Christel Depienne reports no disclosure.

Cas Simons reports no disclosure.

Gajja S. Salomons reports no disclosure.

Fanny Mochel reports no disclosure.

Abstract

Objective: To describe the leukodystrophy caused by pathogenic variants in *LARS2* and *KARS*, encoding mitochondrial leucyl tRNA synthase and mitochondrial and cytoplasmic lysyl tRNA synthase, respectively.

Methods: We composed a group of five leukodystrophy patients, in whom whole genome or whole exome sequencing revealed pathogenic variants in *LARS2* or *KARS*. Clinical information, brain MRIs and post-mortem brain autopsy data were collected. We assessed aminoacylation activities of purified mutant recombinant mitochondrial leucyl tRNA synthase and performed aminoacylation assays on patient's lymphoblasts and fibroblasts.

Results: Patients had a combination of early onset deafness and later onset neurological deterioration caused by progressive brain white matter abnormalities on MRI. Female patients with *LARS2* pathogenic variants had premature ovarian failure. In two patients, MRI showed additional signs of early onset vascular abnormalities. In two other patients with *LARS2* and *KARS* pathogenic variants, MRS revealed elevated white matter lactate, suggesting mitochondrial disease. Pathology in one patient with *LARS2* pathogenic variants displayed evidence of primary disease of oligodendrocytes and astrocytes with lack of myelin and deficient astrogliosis. Aminoacylation activities of purified recombinant mutant leucyl tRNA synthase showed a 3-fold loss of catalytic efficiency. Aminoacylation assays on patient's lymphoblasts and fibroblasts showed about 50% reduction of enzyme activity.

Conclusion: This study adds *LARS2* and *KARS* pathogenic variants as gene defects that may underlie deafness, ovarian failure and leukodystrophy with mitochondrial signature. We discuss the specific MRI characteristics shared by leukodystrophies

caused by mitochondrial tRNA synthase defects. We propose to add aminoacylation assays as biochemical diagnostic tools for leukodystrophies.

Introduction

Leukodystrophies comprise a large group of rare genetic disorders that share abnormal white matter of the brain and spinal cord as central feature.[1,2] With the introduction of whole exome and whole genome sequencing (WES and WGS, respectively), the proportion of patients with unclassified leukodystrophy decreased from 50% in 2010[3] to 20-30% in 2016.[3,4] Strikingly, defects in several specific biological processes were found to be relatively common, including the mitochondrial respiratory chain and the process of translating RNAs into proteins.[3]

These two pathways come together in mitochondrial translation. Aminoacyl tRNA synthases (aaRSs) link amino acids with their cognate tRNAs, a critical step in the translation of messenger RNA into proteins. Except for *KARS* and *GARS* shared by the cytoplasmic and mitochondrial translation machineries, separate sets of aaRSs, encoded by *-ARS* genes, are present in the cytoplasm for the translation of approximately 24,000 nuclear genes, and in the mitochondria, encoded by *-ARS2* genes, for the translation of 13 mitochondria-encoded genes.[5] *DARS2* pathogenic variants were the first identified defect in a mitochondrial aaRS causing Leukodystrophy with Brain stem and Spinal cord involvement and Lactate elevation (LBSL).[6] Subsequently, *EARS2* pathogenic variants were found in Leukodystrophy with Thalamus and Brain stem involvement and Lactate elevation (LTBL),[7] and *AARS2* pathogenic variants in *AARS2*-related ovarioleukodystrophy.[8] Defects in almost all mitochondrial and cytoplasmic aaRSs have been associated with human diseases, often brain disorders or peripheral neuropathies.[9]

In the present paper two more leukodystrophies related to mitochondrial aaRS defects are discussed, caused by pathogenic variants in *LARS2* and *KARS*.

Patients and methods

Patients, approval and consent

Patient 1 was investigated as part of a collaborative Dutch-Australian WGS study to identify the genetic cause in 111 patients from the Amsterdam Database of Unclassified Leukodystrophies. Patients 2-5 underwent diagnostic WES. In all participating centers approval from the institutional ethical committees and written informed consent from patients or guardians were obtained. Affected individuals were examined by neurologists at their primary care centers.

MRI and MRS

We scored all available MRIs according to a standardized protocol.[10] Proton MRS was only assessed for the presence of lactate. Examinations were executed at different MR machines at various field strengths; no attempts at quantification were made, as no comparable results would be obtained.

Brain pathology

Brain tissue from patient 1 was collected at autopsy with a postmortem delay of 6 hours. Formalin-fixed, paraffin-embedded tissue was sectioned at 4 µm and stained for Hematoxylin&Eosin or Kluver-periodic acid Schiff (PAS) according to standard methods. Tissue sections were incubated with antibodies against proteolipid protein (PLP, myelin marker; AbDSerotec, 1:3000), glial fibrillary acidic protein (GFAP, marker of astrocytes; Millipore, 1:1000), CD68 (marker for macrophages and microglia; DAKO, 1:400), neurofilament 70-200 kDa (marker for abnormal axons; Mono, 1:10), and CD45 (marker for lymphocytes; DAKO, 1:100). Negative controls by omitting the primary antibody were included in each experiment. Immunoreactivity

was visualized with secondary antibodies (Envision rabbit/mouse, DAKO) and diaminobenzidine tetrachloride. Sections were counterstained with hematoxylin. Sections were photographed using a Leica DM6000B microscope.

Molecular genetic analyses

In patient 1 and her parents trio WGS was performed on genomic DNA using 2x150 nt paired end reads on an Illumina X (Illumina Cambridge Ltd, Little Chesterford UK). Read alignment was performed using BWA-mem; GATK HaplotypeCaller v3.7 was used for variant calling; SnpEff v4.3m for variant annotation. A custom pipeline was used for variant filtration and prioritisation based on population allele frequency, anticipated inheritance pattern and predicted functional effect of variants.

In patient 2 and parents the coding regions of 4813 genes associated with known phenotypes (TruSight One Illumina panel) were sequenced, processed and analysed as described.[11]

In patient 3 and parents, trio WES analysis was performed as described[12] with the following modifications. Solo whole-exome capture was performed with the SureSelect Clinical Research Exome V1 kit (Agilent, Santa Clara, CA, USA) and libraries were sequenced on a HiSeq 4000 according to the manufacturer's recommendations for paired-end 76 bp reads.

In patient 4, WES was performed DNA using Agilent SureSelectXT Human All Exon 50 Mb kit and sequenced on Illumina HiSeq 2000. Data analysis was performed focussing on a mitochondrial disease gene panel, as previously described.[13]

In patient 5 and parents, trio WES was performed as described previously.[14]

All variants were confirmed by Sanger sequencing.

Aminoacylation assays

Recombinant mtLeuRSs were synthesised to assess aminoacylation of the p.Asn124Ile and p.Arg663Trp variants (identified in patient 2). *LARS2* variants were introduced into the pET22b/*LARS2* construct[15] using site-directed mutagenesis. Wild type and variant *LARS2* were expressed and purified as described.[16] The sequence of *E. coli* $tRNA_5^{Leu}$(UAA) was cloned, transcribed and purified according to established procedures.[17] *In vitro* leucylation of the $tRNA^{Leu}$ transcript was performed in the presence of 30 μM L-[^{14}C]leucine at 37°C, as described.[18] Kinetic parameters were determined from Lineweaver-Burk plots in the presence of 3-30 nM wild type or variant mtLeuRS and concentrations of *E. coli* $tRNA^{Leu}$ transcript ranging from 0.3 to 5.6 μM. Experimental errors for k_{cat} and K_m varied by ≤20%. Data were expressed as averages of at least three independent experiments.

To determine patients' mtLeuRS activity steady state aminoacylation assays were performed in mitochondria from lymphoblasts (kit from Qiagen, Hilden, Germany) following previously published methods.[19] [$^{13}C_2$]-leucine and [$^{13}C_6$,^{15}N]-isoleucine (Cambridge Isotopes, Massachusetts, USA) were used as substrates and [D_3]-leucine as internal standard. Intra-assay coefficient of variation was <15%. MtIleRS activity was used as control. To determine cytosolic LysRS activity steady state aminoacylation assays were performed in fibroblasts under similar conditions, with [D_4]-lysine (Sigma, Germany) as substrate and [$^{13}C_6$]-arginine (Cambridge Isotopes, Massachusetts, USA) as internal standard. All samples were measured in triplicate.

Other studies on mtLeuRS

Immunoblotting and densitometry were performed on patient 2 muscle, as described,[20] with the following modifications: membranes were probed with a 1:250

dilution of anti-mtLeuRS (Abcam ab96221), 1:500 anti-OXPHOS (Abcam ab11041) or a 1:1000 dilution of anti-VDAC1 (Abcam ab14734), overnight at 4°C.

Data availability statement

Anonymized data will be shared by request from any qualified investigator.

Results

Clinical characterization and first laboratory results

All patients are from non-consanguineous families. Family histories were unrevealing, except for patient 5. Pregnancy and delivery were normal or non-contributory in all.

In patient 1, a female, profound congenital sensorineural deafness was diagnosed shortly after birth. Development was somewhat delayed with unsupported walking at 18 months. She learned to speak and use sign language. She graduated from normal level high school and achieved employment in administrative work. She entered premature menopause due to ovarian failure at 29 years. Following a fall at age 33, motor decline set in with cerebellar ataxia and spasticity, left more than right. She developed supranuclear gaze palsy and left-sided central facial palsy. Increasing swallowing difficulties and weight loss prompted PEG tube placement. Pneumonia led to respiratory failure and death at 35½ years. Autopsy was performed.

Patient 2 is a male in whom hypotonia, macrocephaly, and inguinal hernia were noted neonatally. Early development was delayed. He was able to walk unaided at 36 months; his gait remained instable. From 18 months he used hearing aids for sensorineural deafness. He displayed autistic behaviour with hyperactivity and later

also aggression. From age 17 years, he developed atypical seizures with atonic and hypertonic crises, responsive to gabapentin and carbamazepine, but EEGs, including long-term video EEG, did not reveal epileptic activity. Following commencement of neuroleptics he became overweight and developed a metabolic syndrome with hepatic steatosis, mildly raised transaminases and insulin-requiring diabetes mellitus in his twenties. In his thirties, his gait became ataxic. At age 33, he developed a supranuclear gaze palsy and extrapyramidal dysfunction with resting tremor and dystonia. At age 36, he developed acute hemiparesis, ascribed to stroke. Following another stroke at age 37, he became very spastic. At present, he is wheelchair-bound and requires assistance for all activities of daily living.

Patient 3 is a male, who was small for gestational age and hypotonic at birth. Early development was delayed. At age 1½ years, he was diagnosed with profound sensorineural deafness; he received unilateral cochlear implant at 2½ years. At age 4, he displayed episodes of abnormal movements, but EEG did not reveal epilepsy. He developed behavioural problems including hyperkinesia, self-mutilation, temper tantrums and aggression. At present he is 8 years old. His behaviour has improved. He does not speak, but uses sign language. He has mild pyramidal signs with brisk reflexes, but no ataxia. No regression has occurred until now.

Patient 4 is a female, in whom congenital sensorineural deafness was diagnosed. She received a unilateral cochlear implant at 38 years. Early development was normal and she attended normal school. She had her menarche at 16 years, soon followed by amenorrhea. Ovarian failure was diagnosed and hormonal replacement was started. At age 45, she developed right-sided coordination problems. At age 46, she experienced a subacute right-sided weakness with also orientation and concentration problems. Neurological examination revealed pyramidal dysfunction

on the right and some axial ataxia. CT was unrevealing; MRI could not reliably be assessed because of cochlear implant-related artefacts. She experienced further decline and presently, at 48 years, she cannot walk without support because of bilateral spasticity.

Patient 5 is a male, in whom early development was uneventful. He walked unaided at 11 months. At 7 years, he developed sensorineural deafness. He followed special education because of learning difficulties, but could undertake simple professional work. He married and had two children. At 35 years, he became completely deaf. He then developed increasing behavioral and cognitive problems. On neurological examination signs of pyramidal and cerebellar dysfunction were found. His cognitive and motor decline was rapid and he died at age 36 years.

In patients 1 and 4, LH and FSH were high, while oestrogen was low, indicative of ovarian failure. In patient 1 thyroid hormone, TSH, cortisol, ACTH and prolactin were normal. In patient 4, ultrasound revealed streak ovaries. Nerve conduction studies (patients 1 and 2) and electroretinogram (patient 2) were unremarkable.

The patients underwent numerous genetic and metabolic tests, which were unrevealing, except for lactate levels. In patients 1 and 2, CSF lactate was mildly elevated (2.7 mmol/l, upper limit 1.2; and 2.6 mmol/l, upper limit 1.8, respectively). In patients 1-4, blood lactate was normal. In patient 5, lactate was slightly elevated in blood and CSF (1.8 mmol/l and 1.7 mmol/l, respectively, upper limit for both 1.2). Studies focused on mitochondrial respiratory chain defects were unrevealing. Assessment of substrate oxidation rates and activities of individual respiratory chain complexes showed normal results or borderline reductions in mitochondria isolated from muscle (patients 1 and 2), fibroblasts (patient 1) and liver (patient 2). Western blotting revealed no reduction in any of the respiratory chain complexes in

fibroblasts; in muscle a slightly reduced complex I expression was found (patient 2). Sequence analysis of the mitochondrial genome revealed no abnormalities in patients 1, 2 and 4.

Brain MRI and MRS findings

Patient 1 underwent MRIs at 32, 33 and 34 years of age (Fig. 1A). The first MRI showed extensive cerebral white matter abnormalities with partial sparing of directly subcortical and frontal white matter, corpus callosum and anterior limb of the internal capsule. Numerous spots of more normal signal were seen within the abnormal white matter. The posterior limb of the internal capsule and splenium of the corpus callosum were affected. The thalamus contained areas of abnormal signal. Pyramidal tracts and medial lemniscus at the level of the pons were affected. The hilum of the dentate nucleus and an area in the middle cerebellar peduncle on the right had abnormal signal. The cerebellum was slightly atrophic. Two subsequent MRIs showed progression with increasing involvement of frontal white matter and larger parts of the corpus callosum. The right pyramidal tract became affected from motor cortex to pyramid in the medulla, whereas involvement on the left was more limited (Fig. 1A). Diffusion restriction was observed in the pyramidal tract, right more than left (Fig. 1A) and the splenium of the corpus callosum. Some contrast enhancement was present in the right pyramidal tract in the centrum semiovale (Fig. 1A). FLAIR images did not show rarefaction or cystic degeneration. MRS revealed highly elevated lactate in the abnormal white matter (Fig. 1A). Spinal imaging was normal.

Patient 2 underwent MRIs at 24, 32, 36 and 37 years (Fig. 1B). The first MRI showed extensive white matter abnormalities in the parieto-occipital white matter, sparing the

directly subcortical white matter. Numerous spots of more normal signal were seen within the abnormal white matter (Fig. 1B). The posterior limb of the internal capsule was partially affected; corpus callosum and anterior limb were intact. The thalamus, hilum of the dentate nucleus and peridentate white matter contained signal abnormalities (Fig. 1B). The brain stem was spared. There was no cerebellar atrophy and no abnormal enhancement after contrast. The subsequent three MRIs showed progression with increasing involvement of frontal white matter. Thalamic abnormalities increased and basal nuclei became abnormal. Within the abnormal cerebral white matter small cystic lesions appeared with elongated shape, suggesting enlarged perivascular spaces (Fig. 1B). Numerous microbleeds arose in the area of the dentate nucleus and increased over time; the latest MRI also showed microbleeds in the area of the thalamus, basal nuclei and the cerebral hemispheres (Fig. 1B). Multiple small areas of diffusion restriction were seen spread over the cerebral hemispheric white matter at age 36, which had disappeared at age 37, leaving behind small cystic spaces, compatible with lacunar infarctions (Fig. 1B). MRS revealed no lactate.

In patient 3, MRI at age 3 years was normal. MRS was not obtained.

In patient 4, MRI at age 46 years revealed extensive cerebral white matter abnormalities with multiple small cystic spaces, either lacunar infarctions or enlarged perivascular spaces. The thalamus contained signal abnormalities. Anterior and especially posterior limbs of the internal capsule, and pyramidal tracts and medial lemniscus in the brainstem were affected. Images were deteriorated due to artefacts related to the cochlear implant. MRS was not obtained.

In patient 5, MRIs were obtained at 35 and 36 years (Fig. 1C). Sagittal T2-weighted images revealed involvement of the anterior segment and splenium of the corpus

callosum and cerebellar atrophy. The axial images revealed abnormal signal in the frontal and parieto-occipito-temporal white matter, sparing the segment in between. The anterior limb of the internal capsule, fronto-pontine tracts and parieto-occipito-temporo-pontine tracts were affected over their entire extent in the brainstem up to the level of the pons. Areas of diffusion restriction were present within the abnormal white matter. There was no abnormal contrast enhancement. MRS revealed highly elevated lactate in the abnormal white matter. Spinal imaging revealed no abnormalities.

Autopsy findings

Brain weight of patient 1 was normal (1200 gr); external inspection was unremarkable. On coronal cut (Fig. 2A), lateral ventricles were slightly enlarged. Cerebral white matter was inhomogeneous in color and consistency, partly gray and gelatinous, partly white and firm-elastic (Fig. 2B and C). There were no stroke-like lesions or hemorrhages.

Microscopic examination of the cerebral hemispheres revealed inhomogeneously pale white matter with rarefaction to cystic degeneration of periventricular and deep white matter and relative sparing of U-fibers (Fig. 2D-F). There was lack of myelin; remaining myelin sheaths displayed intramyelinic edema and some blebbing. In most affected areas oligodendrocytes were decreased in number. Reactive astrocytes were locally seen, sometimes clustered around blood vessels; reactive gliosis was meagre compared to the degree of tissue damage (Fig. 2H). At the edge of the areas of severe damage, reaching the better preserved U-fibers, astrocytes had gemistocytic morphology with ample eosinophilic cytoplasm, in which round and elongated inclusions were appreciable that were immunoreactive for GFAP.

Throughout the white matter, scattered CD68-positive macrophages were visible and few activated microglia without signs of active myelin breakdown (Fig. 2J). In the areas without myelin, uncovered axons were present together with some spheroids, especially in long tracts (Fig. 2K). There were no infiltrates of inflammatory cells or abnormalities of blood vessel walls. Occasional hemosiderin-containing or weak Oil-red-O-positive macrophages were seen in perivascular spaces. The white matter of the U-fibers was more cellular with increased numbers of cells with morphology of oligodendrocytes or oligodendrocyte progenitors (Fig. 2L). The neocortex was normal without loss of neurons or myelin.

The internal and external capsules showed loss of myelin and reactive gliosis. In the thalami moderate tissue rarefaction was accompanied by reactive gliosis and mild loss of neurons. The basal nuclei displayed only slight decrease in the number of larger neurons in the neostriatum. Pituitary gland, hypothalamus and hippocampus were not affected.

In the brainstem, pyramidal tracts showed variable lack of myelin and axons and numerous axonal spheroids, especially in the midbrain. Neuronal loss in gray matter structures was at most mild.

Cerebellar white matter, especially the hilum of the dentate nucleus, showed lack of myelin, intramyelinic edema and astrogliosis. Cerebellar cortex showed inhomogeneous loss of neurons in granular and Purkinje cell layers accompanied by reactive Bergmann gliosis and some macrophages.

Genetic analysis identifies LARS2 and KARS as candidate genes

WGS in patient 1 identified biallelic heterozygous variants in *LARS2* (NM_015340.3): c.462delT (p.Lys155Asnfs*3) and c.1120A>C (p.Ile374Leu). WES identified biallelic

heterozygous *LARS2* variants c.371A>T (p.Asn124Ile) and c.1987C>T (p.Arg663Trp) in patient 2, c.516G>T (p.Arg172Ser) and c.1028C>T (p.Thr343Met) in patient 3, and c.683G>A (p.Arg228His) and c.880G>A (p.Glu294Lys) in patient 4. In patient 5, WES revealed biallelic heterozygous variants in *KARS* (NM_001130089.1): c.323G>A (p. Arg108His) and c.1426G>T (p. Val476Phe). For patients 1, 2, 3 and 5, both parents were carriers of one of the variants. For patient 4, the mother carried the c.683G>A variant; the father was not available for testing.

All mutations were predicted to be damaging to protein function and all mutations were absent or very rare in gnomAD with no homozygotes reported (Table 1). When comparing the phenotype of our patients, as well as patients from the literature, to their *LARS2* or *KARS* genotype, we did not find clear genotype-phenotype correlations (Fig. 3).

LARS2 and KARS expression profiles

To gain insights into factors possibly accounting for variable phenotypic expression, we assessed expression profiles of *KARS* and *LARS2* using the GTEx and Brainspan resources.[21] Interestingly, *KARS*, and to a lesser degree *LARS2*, showed lowest expression levels in brain tissue from adult individuals (GTEx database). Expression was highly variable for both genes from one individual to the other in the normal population.

Functional analyses of LARS2 and KARS variants

The mtLeuRS protein has been cloned and expressed in *E. coli* with a C-terminal 6-His Tag, purified to homogeneity higher than 95% and shown to be active in the aminoacylation of *E. coli* $tRNA^{Leu}$.[16,22] We measured *in vitro* aminoacylation activities

of purified recombinant mtLeuRS p.Asn124Ile and p.Arg663Trp variants, observed in patient 2, by the incorporation of [^{14}C]-leucine into an *E. coli* tRNA^{Leu} substrate. These variants demonstrated a 3-fold loss of catalytic efficiency (Table 2).

MtLeuRS protein is 903 amino acids in length and contains a mitochondrial signal sequence comprising the first 39 amino acids.[15] Variant p.Asn124Ile is located in the catalytic domain and variant p.Arg663Trp at the interphase between the catalytic and tRNA-binding domains of mtLeuRS (Fig. 3). The crystal structure of both *T. thermophilus* LeuRS[23] and *E. coli* LeuRS[24] complexed to its cognate tRNA suggests that neither of these residues is in direct contact with ATP, leucine or the tRNA substrates, although p.Arg663Trp is strictly conserved in all bacterial-like LeuRSs. In agreement, we found that neither p.Asn124Ile nor p.Arg663Trp mtLeuRS mutants affect tRNA binding to mtLeuRS, as shown by constant K_M values. So the 3-fold efficiency losses are mainly the result of decreased aminoacylation rate (k_{cat}).

In mitochondria isolated from lymphoblasts of patients 2-4, mtLeuRS activity was assessed and compared with mitochondria from three unaffected cell lines, using mtIleRS activity as control (Fig. 4A). MtLeuRS activity was 41-45% of average control values (Fig. 4B). Cytosolic LysRS activity in fibroblasts of patient 5, harbouring *KARS* mutations, showed 52% residual activity compared to controls (Fig. 4B). No lymphoblasts were available to assess mtLysRS activity.

Western blotting

Immunoblotting of mtLeuRS from patient 2 muscle showed reduced levels compared to age-matched controls, while no significant differences were observed in muscle respiratory chain complex levels (Fig. 5). Immunoblotting of fibroblasts from patient 2

showed no change in mtLeuRS protein level and no effect on mitochondrial respiratory chain complex protein levels relative to control fibroblasts (Fig. 5).

Discussion

In this paper we present five patients with leukodystrophy and deafness, related to *LARS2* or *KARS* pathogenic variants. Apart from the cerebral hemispheric white matter, the corpus callosum is affected, connecting the abnormalities on both sides. The leukodystrophy is characterized by long tract involvement, in *LARS2*-mutated patients especially the pyramidal tracts, and in the *KARS*-mutated patient especially the fronto-pontine and parieto-occipito-temporo-pontine tracts. Leukodystrophies caused by mitochondrial tRNA synthase defects (*AARS2, DARS2, EARS2, KARS* and *LARS2*) share certain features. The pattern seen in the *KARS*-mutated patient is similar to that seen in the leukodystrophy caused by *AARS2* pathogenic variants.[8] Interestingly, long tract involvement is also a typical feature of LBSL caused by *DARS2* mutations.[6] The consistent thalamus involvement is shared by the diseases caused by *LARS2* and *EARS2* pathogenic variants.[7] All these disorders share a mitochondrial signature on MRI with often lactate elevations within the abnormal white matter in MRS, while blood and CSF lactate is normal or borderline.[6-8] Areas of diffusion restriction within the abnormal white matter on MRI suggest myelin micro-vacuolization, a feature of mitochondrial leukoencephalopathies.[7,8,25] Distinct features for *LARS2* pathogenic variants, seen in patients 2 and 4, both with clinically manifest strokes, are signs of a vasculopathy, with microbleeds, highly enlarged perivascular spaces and lacunar infarctions. In leukodystrophies, earlier disease onset is generally associated with more rapid decline than later disease onset.[26] In *AARS2-, LARS2* and *KARS*-related disease, however, limited disease signs may be

present from early childhood, followed in adulthood by rapid decline over the course of a few years. Unlike other leukodystrophies including mitochondrial leukodystrophies, we did not identify any precipitating factors in our patients, except for a head trauma in patient 1.

The leukodystrophy caused by *LARS2* pathogenic variants is novel. *LARS2* encodes mitochondrial leucyl-tRNA synthase (mtLeuRS), which is dedicated to the charging of mitochondrial $tRNA^{Leu}$. *LARS2* variants have previously been associated with infantile multi-system disease[27] and Perrault syndrome.[28] *KARS* encodes lysyl-tRNA synthase (LysRS) that aminoacylates $tRNA^{Lys}$ in the cytosol or mitochondria, the cytoplasmic and mitochondrial isoforms resulting from alternative splicing. *KARS* variants have been associated with hypertrophic cardiomyopathy, deafness, peripheral neuropathy[29-32] and recently also leukodystrophy.[33,33] In one paper calcium deposits in addition to white matter abnormalities were reported in brain and spinal cord[31], not observed in patient 5. Although the distribution of the white matter abnormalities was not described in detail, the figures suggest a similar distribution as observed in patient 5, indicating a consistent *AARS2*-like pattern,[8] with the exception of absence of spinal cord abnormalities in our patient.

Pathology of patient 1 shows a widespread loss of oligodendrocytes, correlating with profound lack of myelin. The affected white matter displays cystic degeneration, seen on some MRIs, and intra-myelinic edema, confirming diffusion imaging findings. Astrocytes are affected, with lack of proper reactive gliosis and presence of GFAP-positive intra-cytoplasmic inclusions, suggesting deranged cytoskeletal intermediate filament network, which could explain the meagre reactive gliosis, disproportional to the degree of tissue damage.[34] This is similar to findings in Vanishing White Matter and Alexander disease astrocytes.[1] Taken together, these data suggest a combined

primary involvement of oligodendrocytes and astrocytes in *LARS2*-related leukodystrophy. Patient 1 did not have strokes and brain autopsy did not reveal vascular pathology. It is therefore not possible to speculate about the origin of the early-onset vascular pathology in patients 2 and 4. The axonal spheroids are probably a secondary phenomenon. Individual leukodystrophies are each characterized by specific findings.[26,35] The above pathology is specific of *LARS2*-related leukodystrophy. Metachromatic leukodystrophy, Krabbe disease and X-linked adrenoleukodystrophy show active demyelination with abundant myelin debris and macrophages. Vanishing white matter displays lack of myelin with abnormal astrocytes and meagre reactive gliosis, but floridly increased numbers of immature oligodendrocytes. Hypomyelinating conditions as Pelizaeus-Merzbacher disease feature lack of oligodendrocytes and myelin, but strongly reactive astrocytes and microglia. Prototypic mitochondrial diseases as Leigh syndrome show loss of tissue due to necrosis, and vascular proliferation, reactive astrogliosis and microgliosis. Megalencephalic leukoencephalopathy with subcortical cysts features intra-myelinic edema, and no reactive gliosis, changes in oligodendrocyte cell density or lack of myelin.

In patient 2, *in vitro* aminoacylation activities of purified recombinant mtLeuRS showed a 3-fold loss of catalytic efficiency. Aminoacylation assays performed on lymphoblasts and fibroblast of patients 2-4 showed about 50% reduction of mtLeuRS and LysRS activity. Given the growing number of leukodystrophies related to -*ARS* and -*ARS2* variants, functional assessment of aaRS activities could be a useful biochemical assay as second line investigation (i.e. after plasma lactate, pyruvate, amino acids, homocysteine, very long-chain fatty acids, cholestanol; urinary organic

acids, sulfatides and sialic acid; and activity of lysosomal enzymes in cells) in patients with leukodystrophies, especially if associated with deafness.

All defects in mitochondrial tRNA synthases affect the same process and one would expect similar disease phenotypes. Considering the housekeeping nature of the affected process, one would expect a multi-system disease. The associated disorders, however, are different. Most may cause a disorder of the central nervous system (*AARS2, CARS2, DARS2, EARS2, FARS2, KARS, LARS2, MARS2, NARS2, PARS2, QARS, RARS2, TARS2, VARS2* and *WARS2*), followed by ovarian failure (*AARS2, HARS2, LARS2*) and deafness (*HARS2, IARS2, LARS2* and *KARS*).[9] Within the central nervous system, the disorders show distinct patterns of structural abnormalities, involving gray and/or white matter, leading to recognizable patterns on MRI. However, mutations in the same gene may also lead to different disorders. For instance, *LARS2* mutations have been associated with multisystem disease, Perrault syndrome, intellectual disability, premature ovarian failure and leukodystrophy,[28,29,37-41,current paper] while *KARS* mutations have been associated with peripheral neuropathy, cardiomyopathy, renal tubular acidosis, anaemia and leukodystrophy.[30-33,42-49,current paper] We did not find evidence of genotype-phenotype correlation. The variability in clinical phenotype may be related to the overall residual enzyme activity, which would depend on the nature and association of the variants found on each allele, but also on the expression of the gene in the affected tissue. We would expect the disorder to mainly affect the tissue where the expression and residual activity are lowest. Interestingly, both genes, especially *KARS*, have the lowest expression in affected tissues including the brain. The individual expression of both *LARS2* and *KARS* appears variable from one individual to the other, also regarding different tissues. So, residual enzyme activity and individual variation in

tissue expression may explain which tissue is most affected. The selective involvement of some specific white matter tracts could be related to the greater effects of some -*ARS2* / -*ARS* mutations in certain cell types, as shown in neuronal cell lines for *DARS2*.[50] Complete loss of function of cytoplasmic and mitochondrial aaRSs is likely incompatible with life and the combination of variants observed in living individuals only leads to a moderate decrease of the tRNA synthase activity, as shown in this study.

We add *LARS2* mutations to the spectrum of gene defects that may underlie deafness, ovarian failure and a distinct leukodystrophy. We demonstrate that *KARS* mutations cause a leukodystrophy that is very similar to the one associated with *AARS2* mutations. We propose aminoacylation assays as biochemical diagnostic tool for leukodystrophies.

Acknowledgements

We are grateful to patients and families for their cooperation. JC would like to thank the Crane and Perkins families for donations to this research. We would like to thank Pr Elisabeth Tournier-Lasserve for fruitful discussion for patient 2. We would like to acknowledge the OrphanOmiX group for providing exome sequencing service for patient 3. We would like to acknowledge the Genome Technology Center at the Radboud UMC and BGI Copenhagen for providing the exome sequencing service for subject 4. The data used for the analyses described in this manuscript were obtained from the GTEx Portal on 03/01/2018 and dbGaP accession number phs000424.vN.pN on 03/01/2018.

Appendix

Name	Location	Role	Contribution
Marjo S. van der Knaap	Amsterdam University Medical Centers, Amsterdam	Author	conception & design of the study, data acquisition & analysis, drafted & reviewed the manuscript
Marianna Bugiani	Amsterdam University Medical Centers, Amsterdam	Author	data acquisition & analysis, drafted & reviewed the manuscript
Marisa I. Mendes	Amsterdam University Medical Centers, Amsterdam	Author	data acquisition & analysis, reviewed the manuscript
Lisa G. Riley	University of Sydney, Sydney	Author	data acquisition & analysis, drafted & reviewed the manuscript
Desiree E.C. Smith	Amsterdam University Medical Centers, Amsterdam	Author	data acquisition & analysis, drafted & reviewed the manuscript
Joëlle Rudinger-Thirion	University hospital of Strasbourg,	Author	data acquisition & analysis, drafted &

	Strasbourg		reviewed the manuscript
Magali Frugier	University hospital of Strasbourg, Strasbourg	Author	data acquisition & analysis, drafted & reviewed the manuscript
Marjolein Breur	Amsterdam University Medical Centers, Amsterdam	Author	data acquisition & analysis, drafted & reviewed the manuscript
Joanna Crawford	University of Queensland, St. Lucia	Author	data acquisition & analysis, reviewed the manuscript
Judith van Gaalen	Radboud University Medical Center, Nijmegen	Author	data acquisition & analysis, reviewed the manuscript
Meyke Schouten	Radboud University Medical Center, Nijmegen	Author	data acquisition & analysis, reviewed the manuscript
Marjolaine Willems	University Hospital of Montpellier, Montpellier	Author	data acquisition & analysis, reviewed the manuscript
Quinten Waisfisz	Amsterdam University Medical Centers,	Author	data acquisition & analysis, drafted &

	Amsterdam		reviewed the manuscript
Frederic Tran Mau-Them	University Hospital of Dijon, Dijon	Author	data acquisition & analysis, reviewed the manuscript
Richard J. Rodenburg	Radboud University Medical Center, Nijmegen	Author	data acquisition & analysis, reviewed the manuscript
Ryan J. Taft	Illumina Inc, San Diego	Author	data acquisition & analysis, reviewed the manuscript
Boris Keren	La Pitié-Salpêtrière University Hospital, Paris	Author	data acquisition & analysis, reviewed the manuscript
John Christodoulou	University of Melbourne, Melbourne	Author	data acquisition & analysis, reviewed the manuscript
Christel Depienne	University Duisburg-Essen, Essen	Author	data acquisition & analysis, reviewed the manuscript
Cas Simons	University of Queensland, St. Lucia	Author	data acquisition & analysis, reviewed the manuscript
Gajja S. Salomons	Amsterdam University Medical Centers,	Author	data acquisition & analysis, reviewed

	Amsterdam	the manuscript
Fanny Mochel	Sorbonne Universités, Paris Author	conception & design of the study, data acquisition & analysis, drafted & reviewed the manuscript

References

1. van der Knaap MS, Bugiani M. Leukodystrophies a proposed classification system based on pathological changes and pathogenetic mechanisms. Acta Neuropathol 2017;134:351-382
2. Vanderver A, Prust M, Tonduti D, et al. Case definition and classification of leukodystrophies and leukoencephalopathies. Mol Genet Metab 2015;114:494-500
3. Kevelam SH, Steenweg ME, Srivastava S, et al. Update on Leukodystrophies; A Historical Perspective and Adapted Definition. Neuropediatr 2016;47:349-354
4. Vanderver A, Simons C, Helman G, et al. Whole Exome Sequencing in patients with white matter abnormalities. Ann Neurol 2016;79:1031-1037
5. Yao P, Fox PL. Aminoacyl-tRNA synthetases in medicine and disease. EMBO Mol Med 2013;5:332-343
6. Scheper GC, van der Klok T, van Andel RJ, et al. Mitochondrial aspartyl-tRNA synthetase deficiency causes leukoencephalopathy with brain stem and spinal cord involvement and lactate elevation. Nat Genet 2007;39:534-539
7. Steenweg ME, Ghezzi D, Haack T, et al. Leukoencephalopathy with thalamus and brainstem involvement and high lactate 'LTBL' caused by EARS2 mutations. Brain 2012;135:1387-1394
8. Dallabona C, Diodato D, Kevelam SH, et al. Novel (ovario) leukodystrophy related to AARS2 mutations. Neurology 2014;82:2063-2071
9. Meyer-Schuman R, Antonellis A. Emerging mechanisms of aminoacyl-tRNA synthetase mutations in recessive and dominant human disease. Hum Mol Genet 2017;26(R2):R114-R127

10. van der Knaap MS, Breiter SN, Naidu S, Hart AA, Valk J. Defining and categorizing leukoencephalopathies of unknown origin: MR imaging approach. Radiology 1999;213:121-133
11. Chérot E, Keren B, Dubourg C, et al. Using medical exome sequencing to identify the causes of neurodevelopmental disorders: Experience of 2 clinical units and 216 patients. Clin Genet 2018;93:567-576
12. Thevenon J, Duffourd Y, Masurel-Paulet A, et al. Diagnostic odyssey in severe neurodevelopmental disorders: toward clinical whole-exome sequencing as a first-line diagnostic test. Clin Genet 2016;89:700-707.
13. Wortmann SB, Koolen DA, Smeitink JA, et al. Whole exome sequencing of suspected mitochondrial patients in clinical practice. J Inherit Metab Dis 2015;38:437-443.
14. Bouman A, Waisfisz Q, Admiraal J, et al. Homozygous DMRT2 variant associates with severe rib malformations in a newborn. Am J Med Genet A 2018;176:1216-1221
15. Yao YN, Wang L, Wu XF, Wang ED. The processing of human mitochondrial leucyl-tRNA synthetase in the insect cells. FEBS Lett 2003;534:139-142
16. Yao YN, Wang L, Wu XF, Wang ED. Human mitochondrial leucyl-tRNA synthetase with high activity produced from Escherichia coli. Protein Expr Purif 2003;30:112-116
17. Perret V, Garcia A, Grosjean H, et al. Relaxation of transfer RNA specificity by removal of modified nucleotides. Nature 1990; 344: 787-789
18. Sohm B, Frugier M, Brulé H, et al. Towards understanding human mitochondrial leucine aminoacylation identity. J Mol Biol 2003; 328: 995-1010
19. Mendes MI, Gutierrez Salazar M, Guerrero K, et al. Bi-allelic Mutations in EPRS, Encoding the Glutamyl-Prolyl-Aminoacyl-tRNA Synthetase, Cause a Hypomyelinating Leukodystrophy. Am J Hum Genet 2018;102:676-684

20. Riley L, Menezes MJ, Rudinger-Thirion J, et al. Phenotypic variability and identification of novel YARS2 mutations in YARS2 mitochondrial myopathy, lactic acidosis and sideroblastic anaemia. Orphanet J Rare Dis 2013;8:193-203
21. Miller JA, Ding SL, Sunkin SM, et al. Transcriptional landscape of the prenatal human brain, Nature 2014;508:199-206
22. Bullard JM, Cai YC, Spremulli LL. Expression and characterization of the human mitochondrial leucyl-tRNA synthetase. Biochim Biophys Acta 2000;1490:245-58.
23. Cusack S, Yaremchuk A, Tukalo M. The 2 A crystal structure of leucyl-tRNA synthetase and its complex with a leucyl-adenylate analogue. EMBO J 2000;19:2351-2361
24. Palencia A, Crepin T, Vu MT, et al. Structural dynamics of the aminoacylation and proofreading functional cycle of bacterial leucyl-tRNA synthetase. Nat Struct Mol Biol 2012;19:677-684
25. Steenweg ME, Pouwels PJ, Wolf NI, et al. Leucoencephalopathy with brainstem and spinal cord involvement and high lactate: quantitative magnetic resonance imaging. Brain 2011;134:3333-3341
26. Van der Knaap MS, Valk J. Magnetic resonance of myelination and myelin disorders. 3rd edition. Heidelberg, Springer, 2005
27. Riley LG, Rudinger-Thirion J, Schmitz-Abe K, et al. *LARS2* variants associated with hydrops, lactic acidosis, sideroblastic anemia, and multisystem failure. JIMD Rep 2016;28:49-57.
28. Kosaki R, Horikawa R, Fujii E, Kosaki K. Biallelic mutations in *LARS2* can cause Perrault syndrome type 2 with neurologic symptoms. Am J Med Genet 2018;176:404-408

29. McLaughlin HM, Sakaguchi R, Liu C, et al. Compound heterozygosity for loss-of-function lysyl-tRNA synthetase mutations in a patient with peripheral neuropathy. Am J Hum Genet 2010;87:560-566
30. Verrigni D, Diodato D, Di Nottia M, et al. Novel mutations in *KARS* cause hypertrophic cardiomyopathy and combined mitochondrial respiratory chain defect. Clin Genet 2017;91:918-923
31. Santos-Cortez RL, Lee K, Azeem Z, et al. Mutations in KARS, encoding lysyl-tRNA synthetase, cause autosomal-recessive nonsyndromic hearing impairment DFNB89. Am J Hum Genet 2013;93:132-140
32. Zhou XL, He LX, Yu LJ, et al. Mutations in *KARS* cause early-onset hearing loss and leukoencephalopathy. Hum Mutat 2017;38:1740-1750
33. Ardissone A, Tonduti D, Legati A, et al. *KARS*-related diseases, progressive leukoencephalopathy with brainstem and spinal cord calcifications as new phenotype. Orphanet J Rare Dis 2018;13:45
34. Middeldorp J, Hol EM. GFAP in health and disease. Progress Neurobiol 2011;93:421-443
35. Van der Knaap MS, Bugiani M. Leukodystrophies: a proposed classification system based on pathological changes and pathogenetic mechanisms. Acta Neuropathol 2017;134:351-382
36. Demain LA, Urquhart JE, O'Sullivan J, et al. Expanding the Genotypic Spectrum of Perrault syndrome. Clin Genet 2017;91:302-312
37. Anazi S, Maddirevula S, Faqeih E, et al. Clinical genomics expands the morbid genome of intellectual disability and offers a high diagnostic yield. Mol Psychiatry 2017;22:615-624

38. Zazo Seco C, Wesdorp M, Feenstra I, et al. The diagnostic yield of whole-exome sequencing targeting a gene panel for hearing impairment in The Netherlands. Eur J Hum Genet 2017;25:308-314
39. Soldà G, Caccia S, Robusto M, et al. First independent replication of the involvement of LARS2 in Perrault syndrome by WES of an Italian family. J Hum Genet 2016;61:295-300
40. Pierce SB, Gersak K, Michaelson-Cohen R, et al. Mutations in LARS2, encoding mitochondrial leucyl-tRNA synthetase, lead to POF and hearing loss in Perrault syndrome. Am J Hum Genet 2013;92:614-620
41. Lerat J, Jonard L, Loundon N, et al. An application of NGS for molecular investigations in Perrault syndrome: study of 14 families and review of the literature. Hum Mutat 2016;37:1354-1362
42. Lieber DS, Calvo SE, Shanahan K, et al. Targeted exome sequencing of suspected mitochondrial disorders. Neurology 2013;80:1762-1770
43. Retterer K, Juusola J, Cho MT, et al. Clinical application of whole-exome sequencing across clinical indications. Genet Med 2016; 8:696-704
44. Kohda M, Tokuzawa Y, Kishita Y, et al. A Comprehensive Genomic Analysis Reveals the Genetic Landscape of Mitochondrial Respiratory Chain Complex Deficiencies. PLoS Genet 2016;12:e1005679
45. Verrigni D, Diodato D, Di Nottia M, et al. Novel mutations in KARS cause hypertrophic cardiomyopathy and combined mitochondrial respiratory chain defect. Clin Genet 2017;91:918-923
46. McMillan HJ, Humphreys P, Smith A, S et al. Congenital visual impairment and progressive microcephaly due to lysyl-transfer ribonucleic Acid (RNA) synthetase

(KARS) mutations; the expanding phenotype of aminoacyl-transfer RNA synthetase mutations in human disease. J Child Neurol 2015;30:1037-1043

47. Chen S, Dong C, Wang Q, et al. Targeted Next-Generation Sequencing Successfully Detects Causative Genes in Chinese Patients with Hereditary Hearing Loss. Genet Test Mol Biomarkers 2016;20:660-665

48. Jung J, Lee JS, Cho KJ, et al. Genetic Predisposition to Sporadic Congenital Hearing Loss in a Pediatric Population. Sci Rep 2017;7:45973

49. Murray CR, Abel SN, McClure MB, et al. Novel causative variants in DYRK1A, KARS, and KAT6A associated with intellectual disability and additional phenotypic features. J Pediatr Genet 2017;6:77-83

50. van Berge L, Dooves S, van Berkel CG, et al. Leukoencephalopathy with brain stem and spinal cord involvement and lactate elevation is associated with cell-type-dependent splicing of mtAspRS mRNA. Biochem J 2012;441:955-962

Tables

Table 1. *LARS2*[a] and *KARS(2)*[b] variants with frequency and pathogenicity predictions

Variant cDNA	Variant amino acid	Frequency %[c]	Conservation[d]	SIFT[e]	Polyphen2 (HumVar)[f]	CADD[g]	Mutation Taster[h]
LARS2							
Patient 1							
c.462delT	Lys155Asnfs*3	-	NA	NA	NA	34	disease causing
c.1120A>C	Ile374Leu	-	vertebrates	tolerated	benign	20.8	disease causing
Patient 2							
c.1987C>T	Arg663Trp	0.0012	yeast	deleterious	probably damaging	35	disease causing
c.371A>T	Asn124Ile	-	vertebrates	deleterious	possibly damaging	29.4	disease causing
Patient 3							
c.516G>T	Arg172Ser	0.003	vertebrates	deleterious	possibly damaging	28.2	disease causing
c.1028C>T	Thr343Met	-	vertebrates	deleterious	probably damaging	32	disease causing
Patient 4							
c.683G>A	Arg228His	-	yeast	deleterious	probably damaging	35	disease causing
c.880G>A	Glu294Lys	0.0016	frog	deleterious	probably damaging	25.4	disease causing
KARS(2)							
Patient 5							
c.323G>A	Arg108His	0.0004	yeast	deleterious	possibly damaging	24.9	disease causing
c.1426G>T	Val476Phe	-	yeast	deleterious	benign	34	disease causing

[a] *LARS2* reference sequence NM_015340.3
[b] *KARS(2)* reference sequence NM_001130089.1
[c] Allele frequency from gnomAD r2.0.2 release (http://gnomad.broadinstitute.org/)
[d] Conservation was analyzed in 11 species, including human, chimp, rat, mouse, dog, chicken, frog, tetraodon, fruit fly, *C. elegans*, baker's yeast.
[e] sift.bii.a-star.edu.sg
[f] genetics.bwh.harvard.edu/pph2
[g] cadd.gs.washington.edu; PHRED scaled C-score ranking. Scores above 20 are considered deleterious
[h] mutationtaster.org
NA not applicable

Table 2. Kinetic parameters for leucylation of *E. coli* $tRNA^{Leu}_{(UAA)}$ transcript by wild-type and variant recombinant mtLeuRS

LARS2 variant	K_m (μM)	k_{cat} (min^{-1})	k_{cat}/K_m (min^{-1} μM^{-1} 10^{-3})	Loss of efficiency* (fold change)
WT	0.60	12.0	20.0	1
p.N124I	0.65	4.2	6.5	3.0
p.R663W	0.54	4.0	7.4	2.7

*Loss of efficiency is calculated relative to wild-type (WT) mtLeuRS

Figure legends

Figure 1: MRI of patients with LARS2 and KARS pathogenic variants

A) MRI in patient 1 at 33 years shows extensive cerebral white matter abnormalities with partial sparing of directly subcortical white matter, especially in the frontal region (white arrow heads). Areas of abnormal signal are present in the thalamus (green arrow head) and to a lesser degree the basal nuclei (blue arrow head). Pyramidal tracts in the posterior limb of the internal capsule, midbrain, pons and medulla are affected, right (red arrows) more than left. Spinal cord is normal; cerebellum is slightly atrophic. Diffusion restriction is observed in the pyramidal tract, right (white arrow) more than left, and splenium of the corpus callosum. Some contrast enhancement is present in the right pyramidal tract in the centrum semiovale (white open arrow). MRS reveals highly elevated lactate (doublet at 1.33 ppm, orange arrow) in the abnormal white matter.

B) MRIs in patient 2 at 36 (upper row) and 37 years of age (lower row). The earlier MRI shows extensive cerebral white matter abnormalities, sparing frontal and directly subcortical white matter (white arrow heads). Thalamus (green arrow head), hilum of the dentate nucleus and peridentate white matter (yellow arrow heads) are affected. Small cystic lesions with elongated shape are present, suggesting enlarged perivascular spaces (white arrows). A few foci of diffusion restriction are seen in the centrum semiovale (white open arrows). The later MRI reveals small cystic spaces in the same areas (white open arrows), compatible with lacunar infarctions. The white matter abnormalities have progressed and involve the frontal white matter and entire pyramidal tracts (red arrows). Numerous microbleeds are seen as black dots in the area of the dentate nucleus, thalamus, basal nuclei and cerebral white matter.

C) MRI of patient 5 at 36 years. Sagittal T2-weighted image shows involvement of the genu and splenium of the corpus callosum (white arrows) and cerebellar atrophy. The axial images show abnormal signal in the frontal and parieto-occipito-temporal white matter, sparing the segment in between. The anterior limb of the internal capsule (yellow arrow), fronto-pontine tracts (yellow arrows) and parieto-occipito-temporo-pontine tracts (green arrows) are affected. Areas of diffusion restriction are present within the abnormal white matter. MRS reveals highly elevated lactate (doublet at 1.33 ppm, orange arrow) in the abnormal white matter. N-Acetyl aspartate (2.02 ppm) is close to zero.

Figure 2: Neuropathology of LARS2 leukodystrophy

A) Whole coronal brain slice shows mild dilatation of the lateral ventricles, indicating mild white matter atrophy, and discoloration of the hemispheric white matter with better preservation of the U-fibers. **B, C)** Luxol fast blue- periodic acid Schiff (LFB-PAS, B) and stain against the major myelin protein proteolipid protein (PLP, **C**) of whole mounts of the right cerebral hemisphere show lack of myelin most evident in the deep white matter with relative sparing of the U-fibers. The PLP stain also shows that the lack of myelin has a patchy appearance (arrow). **D)** Hematoxylin&Eosin (H&E) stain of the frontal lobe confirms that the U-fibers are better preserved. **E, F)** FB-PAS and H&E stains of the deep frontal white matter show variable degrees of tissue rarefaction and microcystic degeneration of the tissue. Note the relatively low numbers of oligodendrocytes, as identified by their small, deeply basophilic, round nucleus. **G)** The vacuoles are crossed by PLP-immunopositive strands, indicative of intra-myelinic oedema. **H, I)** Stain against the astrocytic GFAP **(H)** and LFB-PAS **(I)** demonstrate that the degree of reactive gliosis is meagre compared to the tissue

damage and that astrocytes contain GFAP-positive intracytoplasmic inclusions (**H and I, inset**). **J)** Stain against CD68 of the deep parietal white matter shows absence of macrophages and scanty microglial reaction. **K)** Stain against neurofilaments 200KDa (NF) of the frontal lobe shows an axonal spheroid. **L)** H&E stain of the capsula externa shows relative preservation of the tissue with near-normal amounts of myelin and oligodendrocyte numbers. **M)** H&E stain of the midbrain shows microcystic appearance of the white matter of the corticospinal tracts with myelin pallor and reduced oligodendrocytes numbers. **N)** In the same region, NF-positive axonal spheroids are numerous. **O)** H&E stain of cerebellar folium shows loss of cells in the cortical granular layer and of Purkinje cells. The cell density in the molecular layer is near to normal. Original magnifications: D and O, 50X; E-N, 200X.

Figure 3: LARS2 and KARS variants

Schematic representation of the variants identified in this study (in red) or in the literature (in black) on the *KARS* and *LARS2* genes and proteins, and their corresponding phenotypes. Variants identified in this study and previously reported[12-18,35-49] appear in purple. The mutation nomenclature for *KARS* variants is based on the mitochondrial isoform (NM_001130089.1).

Figure 4: Amino-acylation assay

A) MtLeuRS activity normalized to average control cells at 100% of patients (n=3) and controls (n=3) as a group in mitochondria isolated from lymphoblast cell lines. MtIleRS activity is shown as simultaneously measured control enzyme.

B) MtLeuRS activity normalized to average control cells at 100% of individual patients and controls in mitochondria isolated from lymphoblast cell lines. Samples were measured in triplicate, error bars represent SEM.

Figure 5: Immunoblot

Immunoblot analysis of LARS2 and the respiratory chain complexes (I to V) in patient 2 (P2) and age-matched control (C) muscle. VDAC1 was used as a loading control.

Figures

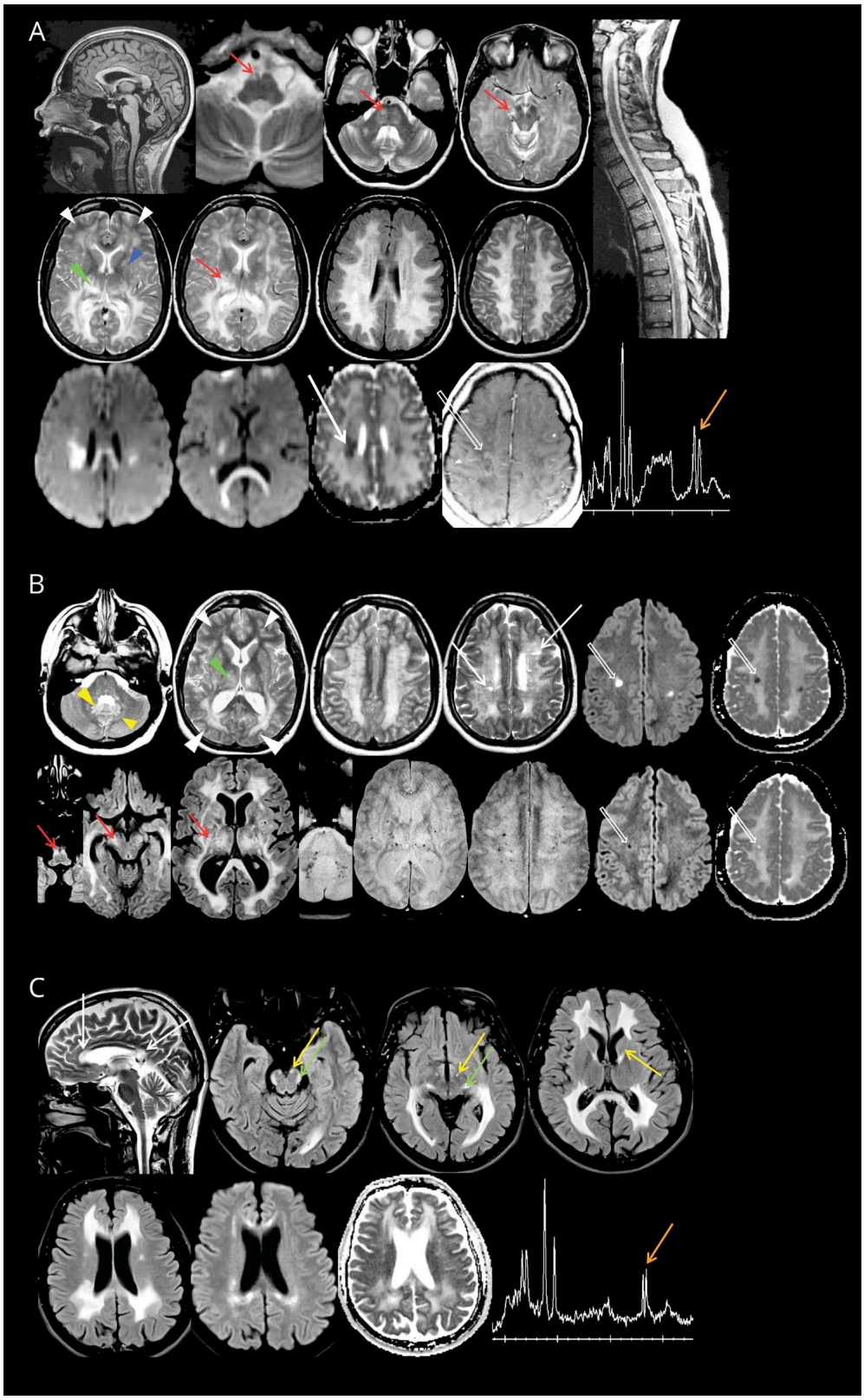

Figure 1

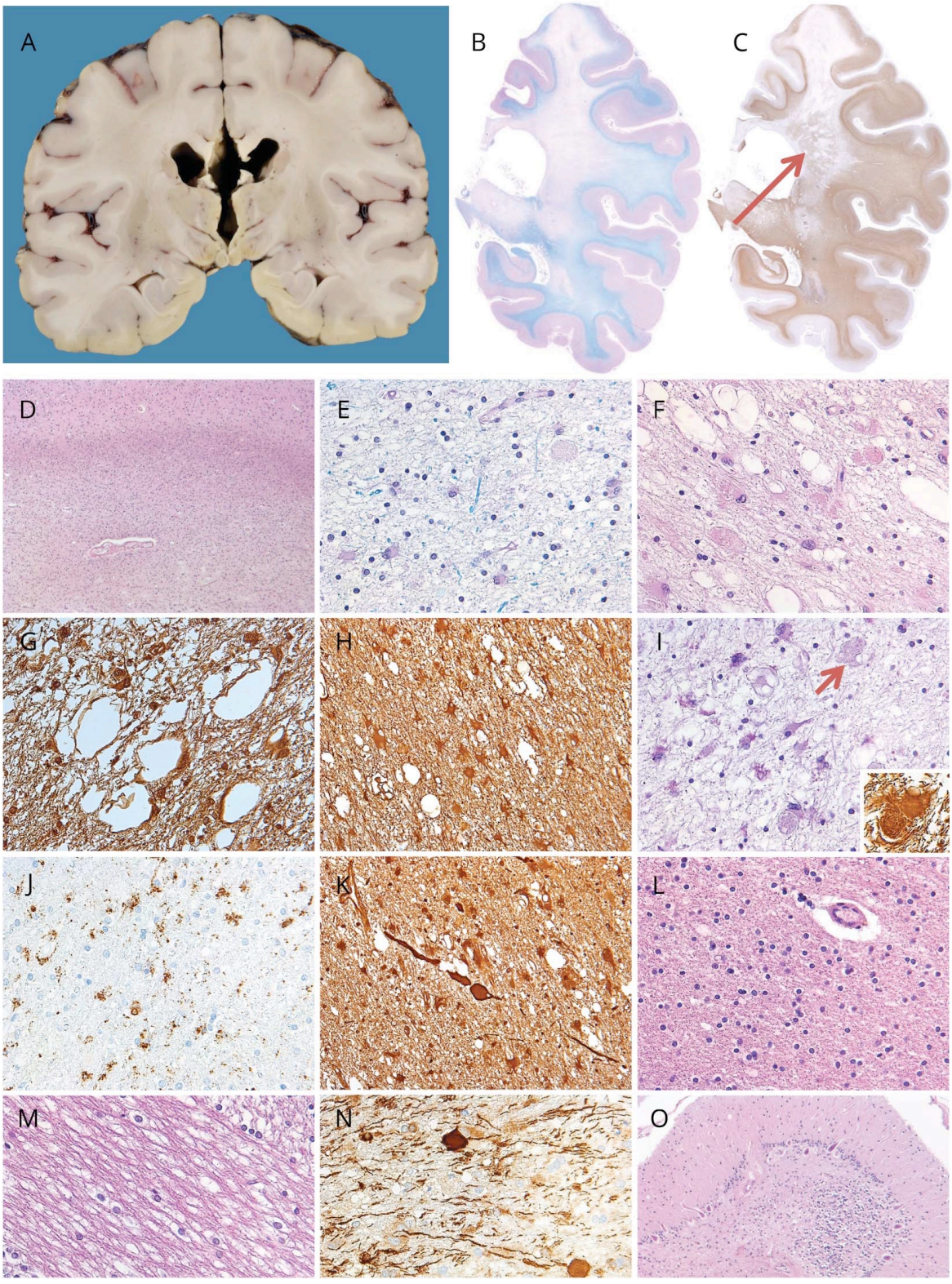

Figure 2

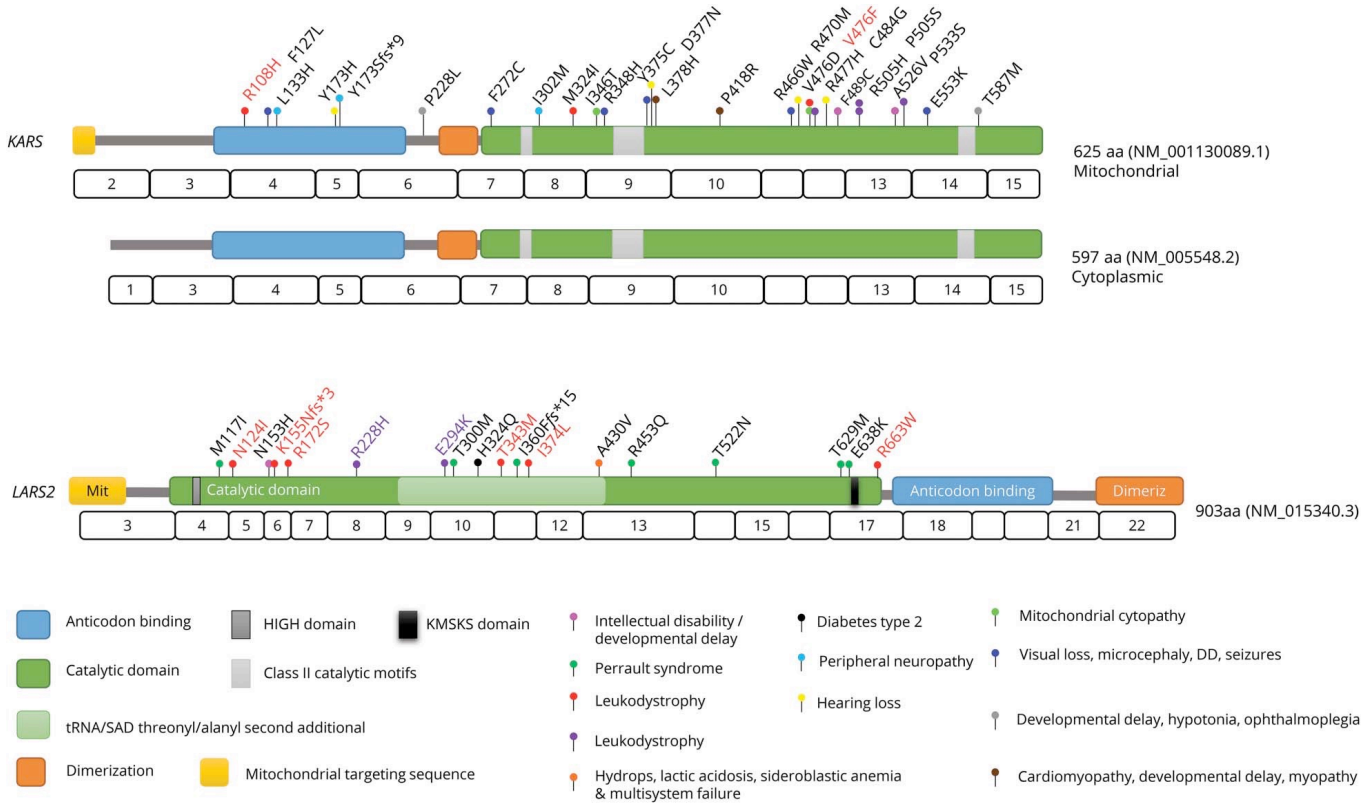
KARS
R108H F127L L133H Y173H Y173Sfs*9 P228L F272C I302M M324I I346T R348H V375C D377N L378H P418R R466W R470M V476D V476F R477H F489C C484G R505H P505S A526V P533S E553K T587M
625 aa (NM_001130089.1)
Mitochondrial
597 aa (NM_005548.2)
Cytoplasmic
LARS2
M117I N124I N153H K155Nfs*3 R172S R228H E294K T300M H324Q T343M I360Ffs*15 I374L A430V R453Q T522N T629M E638K R663W
Mit
Catalytic domain
Anticodon binding
Dimeriz
903aa (NM_015340.3)
Anticodon binding
HIGH domain
KMSKS domain
Catalytic domain
Class II catalytic motifs
tRNA/SAD threonyl/alanyl second additional
Dimerization
Mitochondrial targeting sequence
Intellectual disability / developmental delay
Perrault syndrome
Leukodystrophy
Leukodystrophy
Hydrops, lactic acidosis, sideroblastic anemia & multisystem failure
Diabetes type 2
Peripheral neuropathy
Hearing loss
Mitochondrial cytopathy
Visual loss, microcephaly, DD, seizures
Developmental delay, hypotonia, ophthalmoplegia
Cardiomyopathy, developmental delay, myopathy

Figure 3

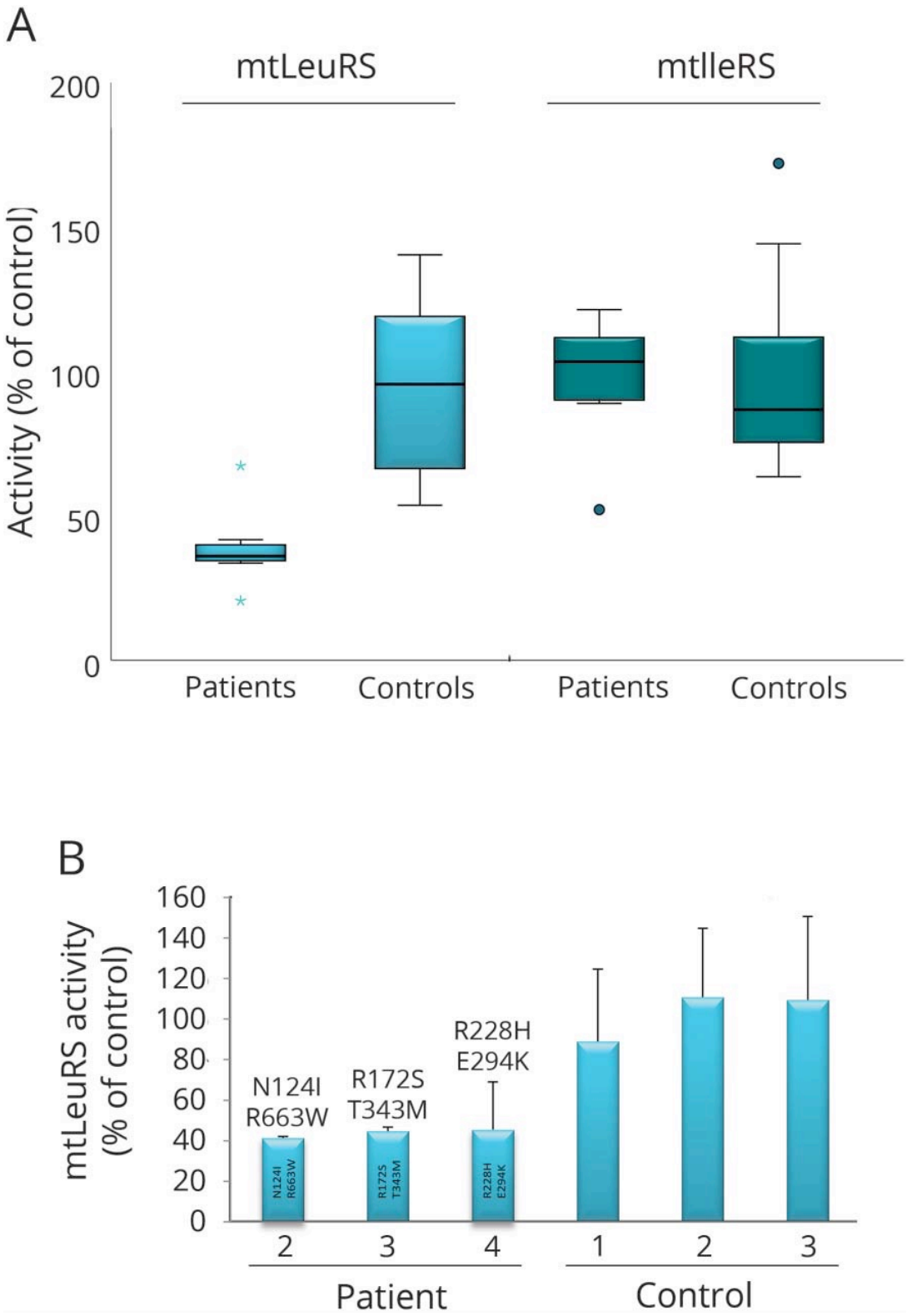
A
mtLeuRS
mtIleRS
Activity (% of control)
200
150
100
50
0
Patients
Controls
Patients
Controls
B
mtLeuRS activity (% of control)
160
140
120
100
80
60
40
20
0
N124I R663W
R172S T343M
R228H E294K
2
3
4
1
2
3
Patient
Control

Figure 4

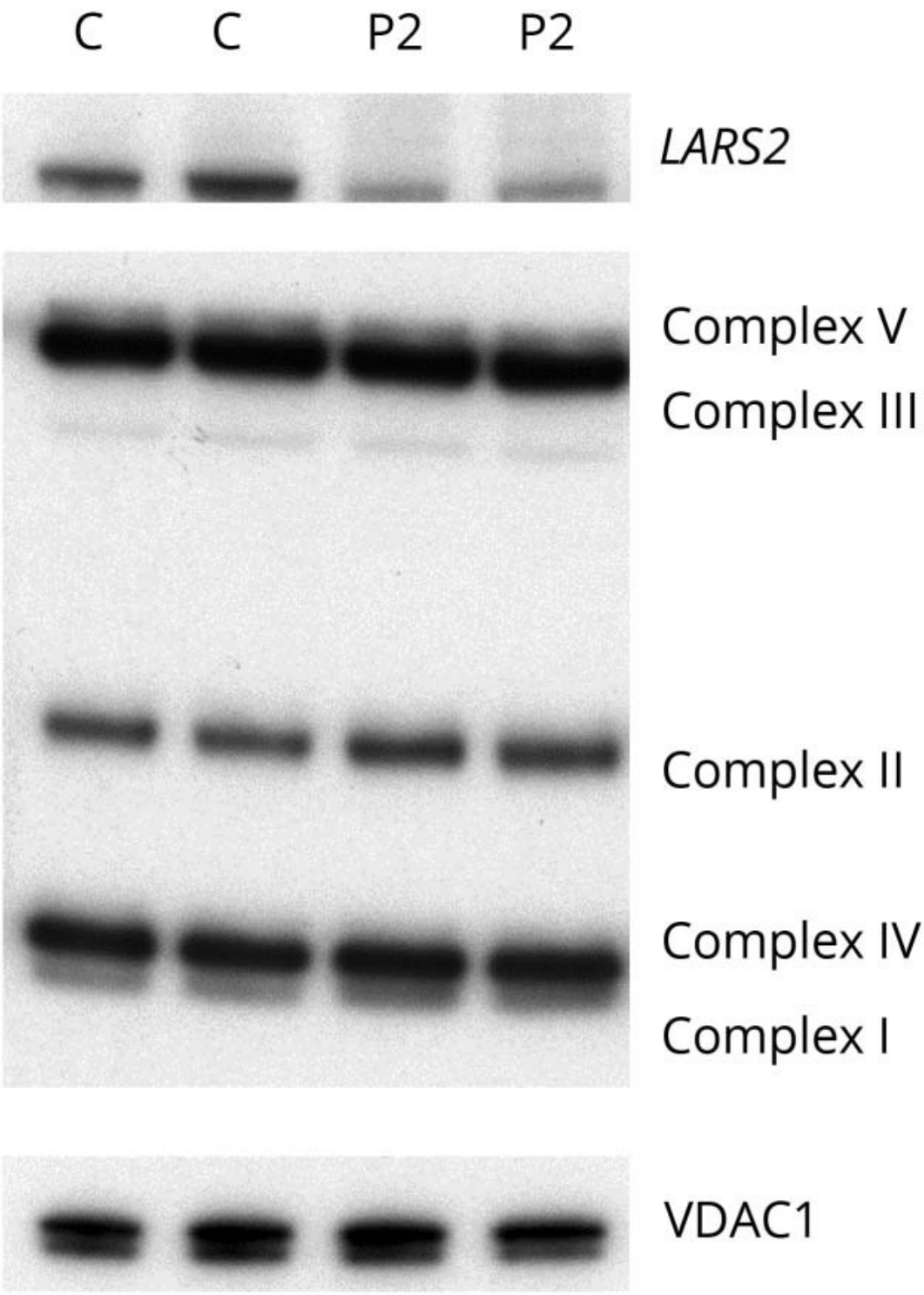
C
C
P2
P2
LARS2
Complex V
Complex III
Complex II
Complex IV
Complex I
VDAC1

Figure 5